JOURNAL OF GUIDANCE, CONTROL, AND DYNAMICS
Vol. 16, No. 4, July–August 1993

Validation of Engineering Methods for Predicting Hypersonic Vehicle Control Forces and Moments

M. Maughmer,* L. Ozoroski,† D. Straussfogel,‡ and L. Long§
Pennsylvania State University, University Park, Pennsylvania 16802

Hypersonic aircraft are being studied for a wide variety of proposed missions. Since the control of these vehicles throughout the speed range has a major impact on their ultimate configuration, it must be considered early in the conceptual design stage. This work examines the ability of the aerodynamic analysis methods contained in an industry standard conceptual design code, the Aerodynamic Preliminary Analysis System, to estimate the forces and moments generated through control surface deflections from low subsonic to high hypersonic speeds. Predicted control forces and moments generated by various control effectors are compared with previously published wind-tunnel and flight-test data for three vehicles: the North American X-15, a hypersonic research airplane concept, and the Space Shuttle Orbiter. Qualitative summaries of the results are given for each force and moment coefficient and each control derivative in the various speed ranges. Results show that all predictions of longitudinal stability and control derivatives are acceptable for use at the conceptual design stage. Results for most lateral/directional control derivatives are acceptable for conceptual design purposes; however, predictions at supersonic Mach numbers for the change in yawing moment due to aileron deflection and the change in rolling moment due to rudder defection are found to be unacceptable for reliable predictions.

Nomenclature

C_D = drag coefficient
C_L = lift coefficient
C_Y = side force coefficient
C_l = rolling moment coefficient
C_m = pitching moment coefficient
C_n = yawing moment coefficient
C_p = pressure coefficient
M_∞ = freestream Mach number
α = angle of attack
γ = ratio of specific heats
δ = local flow deflection angle

Subscripts

a = aileron, asynchronous horizontal tail, or asynchronous elevon deflection (positive, right wing down)
bf = body flap deflection (positive, trailing edge down)
e = elevator or synchronous elevon deflection (positive, trailing edge down)
f = flap deflection (positive, trailing edge down)
h = synchronous horizontal tail deflection (positive, trailing edge down)
v = rudder or vertical tail deflection (positive, trailing edge right)

Introduction

AT the present time, a variety of flight vehicles are being considered for a number of hypersonic missions. Clearly, the development of the flight control systems for these aircraft will have a major impact on their final configurations. Thus, it is important to have methods of predicting flight control forces and moments which are suitable, in both speed and accuracy, for conceptual design efforts. Likewise, because many of the proposed missions include horizontal takeoff from a conventional runway, acceleration to hypersonic and possibly orbital cruise, re-entry and a conventional landing, it is desirable that such methods adequately cover the entire speed range for the vehicle of interest.

Although many different types of subsonic and supersonic analysis methods exist that can predict aerodynamic characteristics, most are not useful for conceptual design due to the long computation times required for analyzing an entire configuration. This becomes increasingly important when considering hypersonic configurations that must operate over an extremely wide range of operating conditions.

A variety of analysis methods are available to predict aerodynamic characteristics at hypersonic Mach numbers. These methods each work well on very specific types of components and Mach number ranges. As a result, when analyzing an entire configuration, the goal is to choose the best combination of these methods for the particular set of analysis conditions.

For the present analysis, a computer code is used which combines a subsonic/supersonic panel method with an impact type finite element analysis for hypersonic speeds. This code, the Aerodynamic Preliminary Analysis System II (APAS II),[1,2] was developed at Rockwell International by integrating a subsonic/supersonic panel program, called the Unified Distributed Panel Method (UDP),[3] with an enhanced version of the Hypersonic Arbitrary Body Program (HABP).[4] This system is capable of evaluating an entire configuration from low subsonic to high hypersonic Mach numbers using a single input geometry base. Typical CPU times on a VAX 8550/VMS range from about 1 min for subsonic or supersonic runs to about 3 min for hypersonic runs with one Mach number, one altitude, and any number of combinations of control surface settings.

The purpose of this work is to examine the ability of the analysis methods contained in APAS II to predict the forces and moments generated through control surface deflections. Since the controllability of hypersonic configurations throughout the speed range has a major impact on acceptable designs, it must be considered early in the conceptual design stage. Thus, the need exists for a fast, reliable way in which to analyze these designs and assess their controllability.

Although HABP has been widely used for conceptual design activities since the early 1970s and a number of studies have been

Presented as Paper 91-2845 at the AIAA Atmospheric Flight Mechanics Conference, New Orleans, LA, Aug. 12–14, 1991; received Sept. 5, 1991; revision received May 8, 1992; accepted for publication Aug. 20, 1992.

*Associate Professor, Aerospace Engineering Department. Senior Member AIAA.

†Graduate Student, Aerospace Engineering Department; currently, Aeronautical Engineer, Lockheed Engineering and Sciences Company. Member AIAA.

‡Graduate Research Assistant, Aerospace Engineering Department. Member AIAA.

§Assistant Professor, Aerospace Engineering Department. Senior Member AIAA.

undertaken to examine its ability to predict the overall vehicle aerodynamics (Refs. 5-9, for example), it is apparent that no comprehensive, systematic study has been conducted to explore its ability to predict forces and moments generated by aerodynamic flight controls. Thus, the goal of the present effort is to determine the accuracy and range of validity of the simple local surface inclination methods for predicting control forces and moments for a variety of configurations

In addition to exploring the validity of the hypersonic capability of APAS, results using the subsonic and supersonic panel methods of that program, including a wetted-area drag prediction, are also compared with experimental data. Although more sophisticated methods are available for predicting control forces and moments in subsonic and supersonic flows, few offer the generality, simplicity, and speed of the panel methods.

The approach taken in this validation effort is to examine several vehicle configurations which cover a broad range of proposed hypersonic vehicle configurations and for which experimental data are available. For each configuration, the theoretical and experimental results are compared across the entire speed range of subsonic, transonic, supersonic, and hypersonic Mach numbers. Details concerning the geometry specification, program implementation, and details of the comparisons between predicted and experimental results are contained in Refs. 10 and 11.

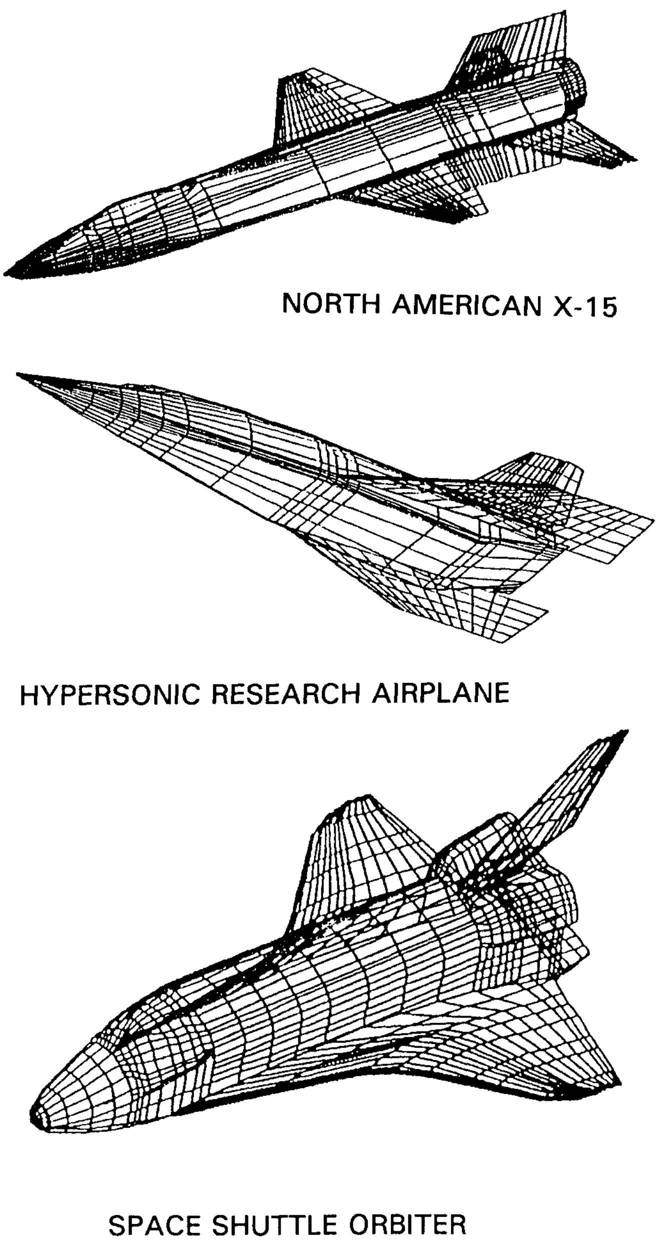

Fig. 1 Hypersonic aircraft used for comparisons of force and moment predictions with experimental results.

Table 1 Hypersonic analysis methods

Impact flow	Shadow flow
Modified Newtonian	Newtonian
Modified Newtonian/ Prandtl-Meyer	Modified Newtonian/ Prandtl-Meyer
Tangent wedge	Prandtl-Meyer empirical
Tangent wedge empirical	OSU blunt body empirical
Tangent cone empirical	Van Dyke unified method
OSU blunt body	High Mach no. base pressure
Van Dyke unified method	Shock expansion method
Blunt body skin friction	Input pressure coefficient
Shock expansion method	Free molecular flow
Free molecular flow	
Input pressure coefficient	
Hankey flat surface empirical	
Delta wing empirical	
Dahlem-Buck empirical	
Blast wave	
Modified tangent code	

Prediction Methods

The theoretical analysis method used for subsonic and supersonic Mach numbers is a version of the Woodward (subsonic-supersonic) panel program called the Unified Distributed Panel Method (UDP).[3] This first-order panel method is capable of analyzing a complete configuration with relatively short computation times. It is based on linear potential flow theory, but includes edge effects and semiempirical techniques for the calculation of skin friction drag. Whereas the effects of leading edge vortices can be modeled in UDP using a Polhamus suction analogy, detailed vortex flowfield predictions require the use of an Euler or Navier-Stokes code. The UDP method is described in detail in Refs. 1 and 2.

At hypersonic speeds, the assumptions made for the linearized potential equation are no longer valid since the perturbation velocities are not small relative to the freestream. In addition, the properties of the flowfield begin to change. Characteristics of hypersonic flow include thin shock layers, strong shock waves, and thick boundary layers. High temperatures occur in the boundary layer, especially in the nose region. Because of these high temperatures, caused by the strong compression of the gas ahead of the body and the heat from the viscous shearing along the body, the gas can dissociate and ionize. Thus, it becomes necessary at these speeds to consider the phenomena occurring in high temperature gases. The ratio of specific heats γ can no longer be assumed to remain constant (equal to 1.4 for air) and becomes a function of temperature and pressure.

Although hypersonic flow is nonlinear and encompasses many unique characteristics, numerous approximate methods have been developed to estimate the resulting pressures on bodies in hypersonic flow. The hypersonic methods used in this analysis are incorporated in an enhanced version of the Hypersonic Arbitrary Body Program.[4] The original was developed in the late 1960s and includes many of the hypersonic analysis methods available today. The geometry of a configuration is represented by a system of quadrilateral panels. The only parameter in the various methods required to calculate each panel pressure is the impact angle of the freestream flow with the panel or the change in impact angle from one panel to another. The various methods included in the program are listed in Table 1.

For each component, various analysis methods can be chosen. Body components are typically broken into two separate regions. The forwardmost body component may have a nose region (if the half angle between the first two cross sections is greater than 30 deg) and a body region. The rearmost body component will have a body region and may have a blunt end region. In each region, an analysis method must be chosen for the impact flow region and another for the shadow flow region.

Table 2 North American X-15, HRA, and Space Shuttle analysis conditions

Configuration	Mach number	Reynolds number	Stag. press., lb/ft^2	Stag. temp., °R	Altitude, ft
NA X-15	0.06	0.40×10^6	2120.9	519.0	0.0
NA X-15	0.80	3.74×10^6	1857.4	526.7	14510.0
NA X-15	1.03	4.12×10^6	1942.6	544.1	19585.0
NA X-15	1.18	4.18×10^6	1989.3	556.4	23420.0
NA X-15	2.96	0.27×10^6	689.3	1129.6	103420.0
NA X-15	4.65	0.41×10^6	6762.0	2187.0	104000.0
NA X-15	6.83	3.27×10^6	55000.0	1135.0	——
HRA	0.20	6.00×10^6	3084.8	234.9	——
HRA	0.80	2.83×10^6	1280.1	490.7	——
HRA	0.98	$3.07. \times 10^6$	1320.8	502.8	——
HRA	1.20	3.17×10^6	1378.8	520.2	——
HRA	6.00	7.44×10^6	63366.0	900.0	——
Space Shuttle	0.25	6.65×10^7	2210.2	525.2	0.0
Space Shuttle	0.80	4.10×10^7	408.6	439.9	48000.0
Space Shuttle	1.20	3.20×10^7	332.9	502.3	62000.0
Space Shuttle	5.00	8.00×10^6	5079.6	2601.5	120000.0
Space Shuttle	20.00	1.26×10^4	12634.4	26957.3	300000.0

An aerodynamic lifting surface is divided into a leading-edge region, a surface region, and possibly a blunt end region if the surface has a finite thickness trailing edge. Again, an impact method and a shadow method must be chosen for each region. The full details of HABP can be found in Refs. 4 and 12. Choosing the most appropriate analysis method for each portion of the vehicle is not trivial and cannot be described in detail here. References 1, 2, 4, 6, 9, and 10 all present guidelines selecting the most suitable analysis methods for any given vehicle and operating condition.

Vehicle Geometries

After reviewing the available experimental data for the aerodynamic characteristics of hypersonic vehicles, three hypersonic aircraft configurations were chosen for study. These are the North American X-15, the hypersonic research airplane (HRA), and the Space Shuttle Orbiter, all shown in Fig. 1. These vehicles cover a broad range of possible hypersonic configurations and are well suited for analysis. The geometries of the configurations chosen are well defined in published reports and there is experimental data available across the entire speed regime. Although many hypersonic vehicle concepts have been studied in the past, few have been tested at subsonic, transonic, supersonic, and hypersonic speeds. The last requirement is that the data include a variety of control deflections. The configurations chosen cover a wide range of control surfaces including those most important for hypersonic flight.

North American X-15

The first configuration to be discussed is the North American X-15, developed in the late 1950s and flown in the early 1960s. The X-15 was designed to reach a velocity of 6600 ft/s and an altitude of 250,000 ft. Wind-tunnel data used for comparison with predicted results are taken from Refs. 13–16. References 17 and 18 present flight-test data that agree well with the wind-tunnel data used here.

The fuselage is basically a circular cylinder in shape with fairings along both sides. The wing has an aspect ratio of 2.5, a quarter chord sweep angle of 25 deg, and is equipped with conventional trailing-edge flaps for use during landing. The horizontal tail has a quarter chord sweep angle of 45 deg and is mounted with 15 deg of anhedral. This all-movable tail is deflected symmetrically for pitch control and asymmetrically for roll control.

For the hypersonic analysis, the impact methods chosen for the various components are: tangent cone empirical for the bodies; tangent wedge empirical for the surfaces; and modified Newtonian for the leading edges, blunt trailing edges, and the blunt end of the fuselage. Prandtl-Meyer empirical is used for all shadow regions except for blunt ends or trailing edges where the high Mach number base pressure method is used. Viscous contributions are calculated using a fully turbulent boundary layer and the reference temperature/Spalding-Chi method.

The analysis conditions for the X-15 runs are given in Table 2. The combination of Mach number and Reynolds number are used to determine the appropriate test conditions. Most of the Mach and Reynolds number combinations correspond to altitudes in the standard atmosphere. For these cases, the Mach number and altitude were input.

Hypersonic Research Airplane

The second configuration to be considered is a proposed wing-body hypersonic research airplane. It was developed at NASA Langley Research Center in the mid-1970s to serve as a hypersonic flight technology demonstrator. Results from wind-tunnel tests on this configuration are reported in Refs. 19–22 for Mach numbers ranging from 0.2 to 6.0.

The configuration consists of a body, a cropped delta wing, and a center vertical tail. The wing is mounted with 2.1-deg negative incidence and 10.0-deg dihedral. It is equipped with full span elevons which can be deflected symmetrically for pitch control and asymmetrically for roll control. The center vertical tail has a dual hingeline that allows for a diamond-shaped airfoil at subsonic and supersonic speeds. At hypersonic speeds, the rear portions deflect to form a wedge-shaped airfoil. They can also be deflected to form speedbrakes at high speeds. The dual hinged rudder can also be deflected in the same direction to provide yaw control.

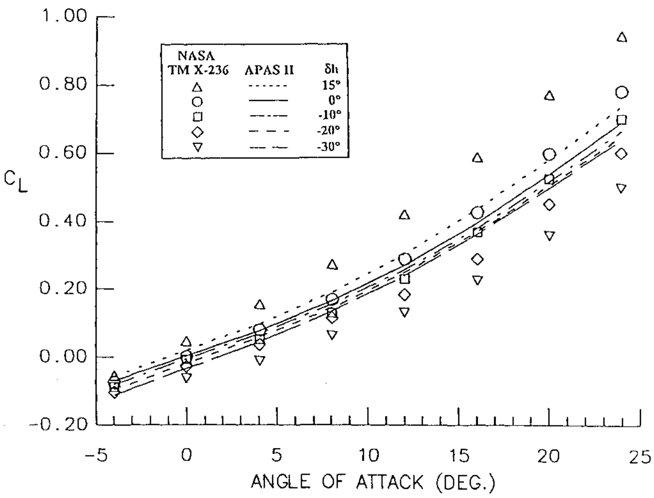

Fig. 2 Comparison of experimental and theoretical lift coefficients for the North American X-15 at Mach 6.83 for various horizontal tail deflections.

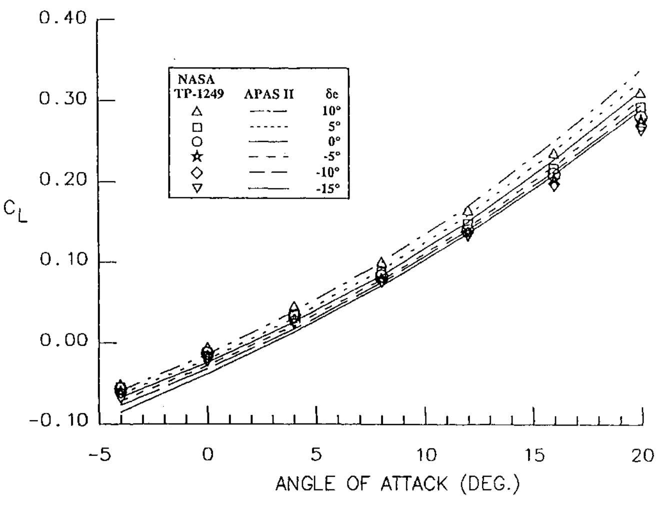

Fig. 3 Comparison of experimental and theoretical lift coefficients for the HRA at Mach 6.0 for various elevon deflections.

The intended propulsion system was a scramjet engine located on the underside of the body. The scramjet is not included in the physical geometry model since most of the experimental data are available for the model both with and without the engine. Not including the engine reduces the complexity of the physical geometry model significantly and has no effect on the analysis of prediction capabilities with regard to control effectors. The experimental data at transonic Mach 8 numbers for roll and directional control do include the scramjet in the model, but are compared to theoretical data without the scramjet. All of the other comparisons are made using experimental data that do not include the engine.

The geometry model used for the hypersonic analysis is identical to that used for the subsonic/supersonic analysis. The viscous contributions to the configuration aerodynamics are calculated using a fully turbulent boundary layer and the reference temperature/Spalding-Chi method. Tangent-cone empirical is the impact method chosen for all body components and Prandtl-Meyer empirical is used as the shadow method. Modified Newtonian flow theory and the high Mach number base pressure are the impact and shadow methods, respectively, used for the blunt end of the last body component. Modified Newtonian is used as the impact method for leading edges and blunt trailing edges of the wing and vertical tail. Tangent-wedge empirical is the impact method used for wing and tail surfaces. Prandtl-Meyer empirical is the shadow method for the leading edges and surfaces, whereas the high Mach number base pressure method is used for the blunt trailing edges.

The analysis conditions for each run were determined by matching the Reynolds number and Mach number at which the experimental data were obtained. The resulting stagnation pressure and temperature, as well as Mach number, were used to set up the theoretical analysis runs. At Mach 6.0, the Reynolds number and Mach number do not correspond to the stagnation pressure and temperature published in the report. In this case, the Reynolds number is disregarded. The analysis conditions for this configuration are given in Table 2.

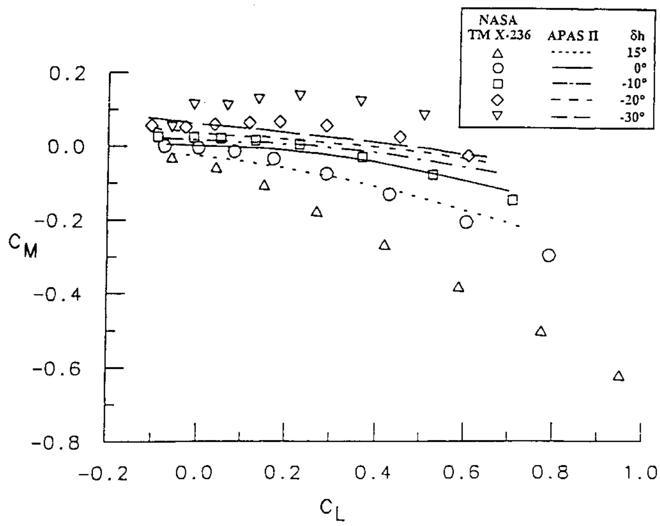

Fig. 6 Comparison of experimental and theoretical pitching moment coefficients for the North American X-15 at Mach 6.83 for various horizontal tail deflections.

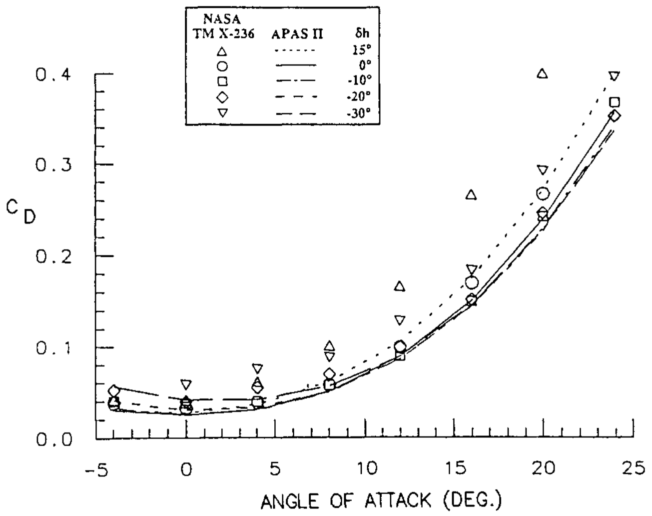

Fig. 4 Comparison of experimental and theoretical drag coefficients for the North American X-15 at Mach 6.83 for various horizontal tail deflections.

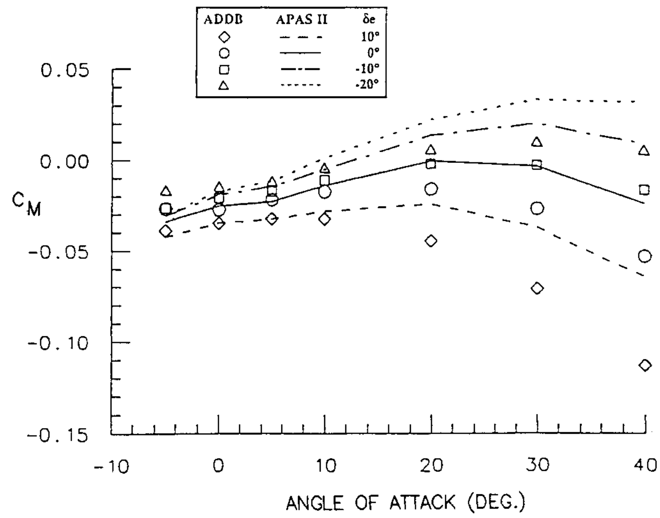

Fig. 7 Comparison of experimental and theoretical pitching moment coefficients for the Space Shuttle Orbiter at Mach 5.0 for various elevon deflections; hypersonic shielding option included in the calculations (ADDB refers to Ref. 23).

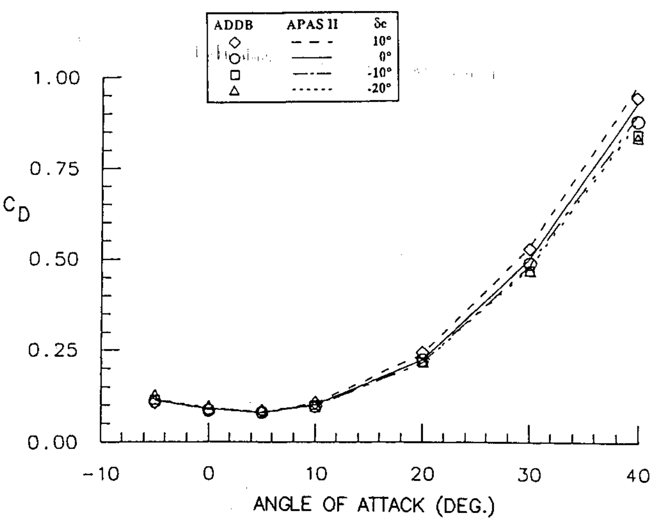

Fig. 5 Comparison of experimental and theoretical drag coefficients for the Space Shuttle Orbiter at Mach 5.0 for various elevon deflections; hypersonic shielding option included in the calculations (ADDB refers to Ref. 23).

Space Shuttle Orbiter

The third configuration analyzed is the Space Shuttle Orbiter. The majority of the aerodynamic data (wind tunnel and flight test) used in the analysis (both wind tunnel and flight) comes from Ref. 23. Although the Space Shuttle has been flying since 1980 (approach and landing tests), and published aerodynamic data exist from the first few flights, the decision was made to use the earlier wind-tunnel-test data in the analysis because it is more complete.

Table 3 Qualitative assessment of the ability of APAS to predict longitudinal stability and control derivatives categorized by speed range

M_∞	C_L	C_{L_α}	$C_{L_{\delta_e}}$	C_D	$C_{D_{\delta_e}}$	C_m	C_{m_α}	$C_{m_{\delta_e}}$
Subsonic $M_\infty < 0.8$	○	○	○	◑	◑	◑	◑	○
Transonic $0.8 < M_\infty < 1.2$	○	○	○	◑	◑	◑	◑	◑
Supersonic $1.2 < M_\infty < 4.5$	○	○	○	○	○	◑	◑	◑
Low hypersonic[a] $4.5 < M_\infty < 8.0$	○	○	○[c]	○	○	◑[b]	◑[b,c]	○[b,c]
High hypersonic[a] $8.0 < M_\infty < 20.0$	○	○	○[c]	◑	○	◑	◑	○

○ Trends predicted well and magnitudes are within 40% over a significant portion of the operating range.
◑ Results should be regarded cautiously: magnitudes near zero angle of attack or trends with angle of attack, but not both, are predicted reasonably well.
● Not useful.

[a]Lateral/directional results are generally better without shielding.
[b]Some problems in predicting results for X-15.
[c]Some problems in predicting results for Space Shuttle Orbiter.

Table 4 Qualitative assessment of the ability of APAS to predict lateral directional control derivatives categorized by speed range

M_∞	$C_{Y_{\delta a}}$	$C_{n_{\delta a}}$	$C_{l_{\delta a}}$	$C_{Y_{\delta v}}$	$C_{n_{\delta v}}$	$C_{l_{\delta v}}$
Subsonic $M_\infty < 0.8$	○[c]	○[c]	○	◑	◑[b]	◑
Transonic $0.8 < M_\infty < 1.2$	○	○	○	◑	◑	◑
Supersonic $1.2 < M_\infty < 4.5$	○	●	◑	○	○	●
Low hypersonic[a] $4.5 < M_\infty < 8.0$	◑[b]	○[b]	○[b]	○[c]	○[c]	○[c]
High hypersonic[a] $8.0 < M_\infty < 20.0$	○	○	○[c]	○	○	○

○ Trends predicted well and magnitudes are within 40% over a significant portion of the operating range.
◑ Results should be regarded cautiously: magnitudes near zero angle of attack or trends with angle of attack, but not both, are predicted reasonably well.
● Not useful.

[a]Lateral/directional results are generally better without shielding.
[b]Some problems in predicting results for X-15.
[c]Some problems in predicting results for Space Shuttle Orbiter.

Flight-test data have been included when available. The Mach numbers tested range from 0.25 to 20.0 at standard trajectory altitudes from sea level to 300,000 ft.

The Orbiter configuration consists of a body, a double delta wing, a body flap, and a center vertical tail. The double delta wing is equipped with full span elevons broken into two panels on each side. These can be deflected symmetrically as an elevator for longitudinal control or asymmetrically as ailerons for roll control. Full span deflections are used in the analysis for all elevator and aileron tests. The body flap, located on the bottom side at the rear of the Orbiter, is used as the primary trim device. Body flap deflections range from +22.5 (positive trailing edge down) to −11.7 deg. The vertical tail consists of a split rudder which can be deflected together for yaw control and separately as a speedbrake.

The model used for the hypersonic analysis is identical to the physical geometry model used for the subsonic/supersonic analysis. The impact and shadow methods used are similar to those of the previous configurations. Viscous contributions are again calculated using a fully turbulent boundary layer and the reference temperature/Spalding-Chi method.

The analysis conditions for the Space Shuttle Orbiter are given in Table 2. The Mach number and Reynolds number combinations are chosen from a typical trajectory and matched with the corresponding standard altitude.

Validation of the Theoretical Methods

To assess the usefulness of the computationally efficient methods discussed in the conceptual design phase of future hypersonic flight vehicles, predictions using these methods have been compared with experimental data for the three vehicles noted. Although the experimental data used are taken primarily from wind-tunnel measurements, a few lateral/directional flight-test results for the Space Shuttle Orbiter are also included.

Longitudinal Aerodynamics

Typical examples of the comparisons between theoretical predictions and experimental results for longitudinal aerodynamics at hypersonic Mach numbers are given in Figs. 2–7. The cases presented were selected to demonstrate the range of the comparisons obtained. They include some of the best agreement found between predicted and experimental results, as well as some of the worst.

The lift curve for the X-15 at a Mach number of 6.83 with different horizontal tail deflections is shown in Fig. 2. It is seen that whereas the flow inclination methods predict the baseline, zero-tail deflection reasonably well, for this configuration the change in lift due to a tail deflection is not well predicted. In contrast, the lift curve, and especially the change in lift with elevon deflection, for the HRA at a Mach number of 6.0, presented in Fig. 3, is predicted very well.

The comparison of drag coefficient as a function of angle of attack predictions with experimental results for the X-15 at a Mach number of 6.83 is shown in Fig. 4. Again, whereas the baseline prediction for this configuration is not bad, the predicted change in drag with horizontal tail deflection, particularly for $\delta_h = +15$ deg, does not agree well with the experimental results. As shown in Fig. 5, better predictions for drag coefficient as a function of angle of attack are obtained for the Space Shuttle Orbiter at a Mach number of 5.0. For this case, as was generally found to be true for predicted drag results, the inclusion of the hypersonic shielding option improves the agreement between the prediction and experiment.

A comparison of predicted and experimental results for pitching moment coefficient vs lift coefficient and control deflection angle is given for the X-15 at a Mach number of 6.83 in Fig. 6. Clearly, for this case the change in moment as it depends on control deflection is not well predicted. As seen in Fig. 7, however, the prediction of similar quantities for the Space Shuttle Orbiter at a Mach number of 5.0 are good. For these predictions, the hypersonic shielding option was not included in the calculations. As a further comparison, the same case with the shielding included is described in Refs. 10 and 24. It is seen, as found in a number of cases, that the pitching moment predictions are better at the higher angles of attack with the hypersonic shielding option not included in the calculations, but slightly better at the lower angles of attack when it is included.

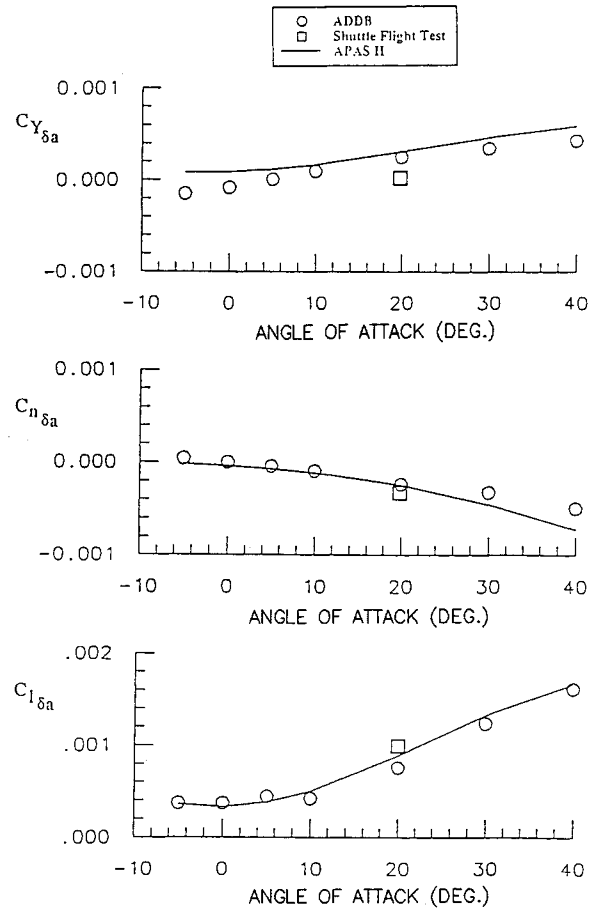

Fig. 8 Comparison of experimental and theoretical increments in lateral force and moment coefficients due to differential elevon deflections for the Space Shuttle Orbiter at Mach 5.0 (ADDB refers to Ref. 23).

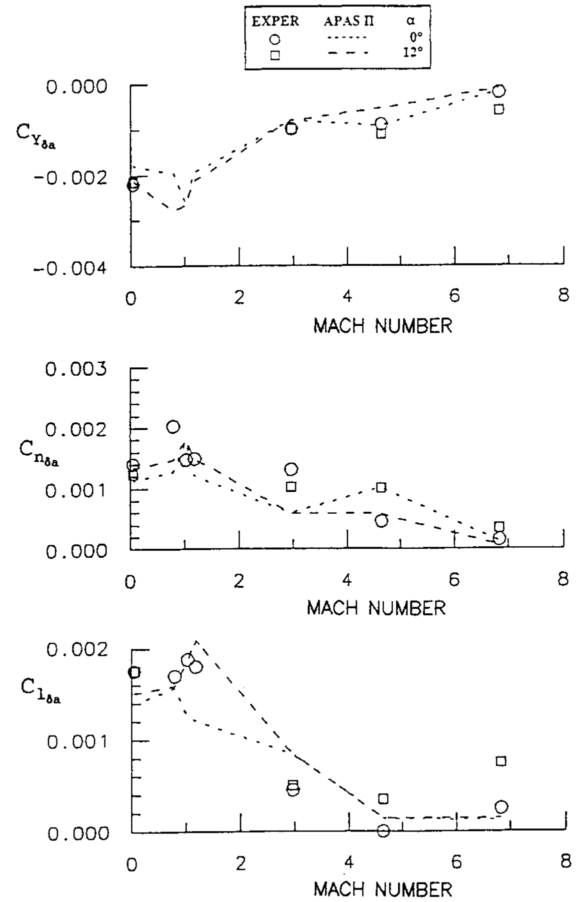

Fig. 9 Comparison of experimental and theoretical increments in lateral force and moment coefficients due to differential horizontal tail deflections as a function of Mach number for the North American X-15.

Comparisons between predicted and experimental results similar to those mentioned, detailed and fully discussed in Refs. 10 and 11, were made for the three vehicles considered at all of the operating conditions given in Table 2. Using these comparisons, a qualitative assessment was made on the suitability of the various methods considered for predicting aerodynamic forces and moments due to flight control effectors. A summary of this assessment for longitudinal quantities is presented in Table 3. It should be emphasized that the evaluation presented in this table is largely the result of personal judgment and should be considered only as a convenient way of summarizing the large quantity of results obtained and to provide rough guidelines for the application of the theoretical methods examined. If one is concerned with a specific application, a more accurate assessment of a particular method would be obtained by considering the case by case comparisons given in Refs. 10 and 11.

The assessment of predicting a particular quantity in a given speed range is based on the following: 1) capable of predicting magnitudes within 40%, as well as the proper trends, over a significant portion of the operating range; 2) capable of predicting trends reasonably well but not magnitudes; and 3) generally unacceptable for conceptual design work.

Briefly, the limitations of UDP for predicting the subsonic/supersonic aerodynamics are related to the fact that there is no accounting for the effects of boundary-layer displacement thickness and flow separation. Whereas this obviously causes problems in predictions made at higher angles of attack, it also is responsible for problems in predicting pitching moments accurately.

At transonic Mach numbers, UDP gives much better results than should be expected. Given that the linearized velocity potential equation is invalid near sonic freestream Mach numbers, it is likely that the results obtained are fortuitous.

For hypersonic flight conditions, HABP does a reasonably good job of predicting the longitudinal aerodynamics. In general, including the effect of shielding in the hypersonic predictions results in only a slight increase in agreement for lift and pitching moment but a significant increase in agreement for drag predictions. Thus, in the interest of time and accuracy, shielding should only be included in the analysis when drag predictions are desired.

Lateral/Directional Aerodynamics

Typical comparisons between predicted and experimental lateral/directional aerodynamics are given in Figs. 8–10. The changes in lateral/directional force and moment coefficients due to a differential elevon deflection as a function of angle of attack for the Space Shuttle Orbiter at a Mach number of 5.0 are presented in Fig. 8. The predictions agree well with the experimental data, including the flight-test result. Summary plots of lateral/directional force and moment coefficients due to a differential tail deflection as a function of Mach number are given for the X-15 in Fig. 9. For the most part, the predictions of UDP and HABP agree reasonably well with the experimental data.

The change in lateral/directional force and moment coefficients due to directional control deflections were not found to be, in general, as good as those due to lateral control deflections. This is demonstrated by the summary plots of the change in force and moment coefficients due to rudder deflections at various Mach numbers for the HRA shown in Fig. 10. Whereas the predictions obtained with HABP at $M_\infty = 6$ are good, those obtained with UDP at subsonic and supersonic Mach numbers are not. Somewhat better are similar summary plots for the Space Shuttle Orbiter presented in Ref. 10. In this case, HABP results are again in good agreement with experimental results, whereas the trends, and to a certain extent the actual values of the stability derivatives, pre-

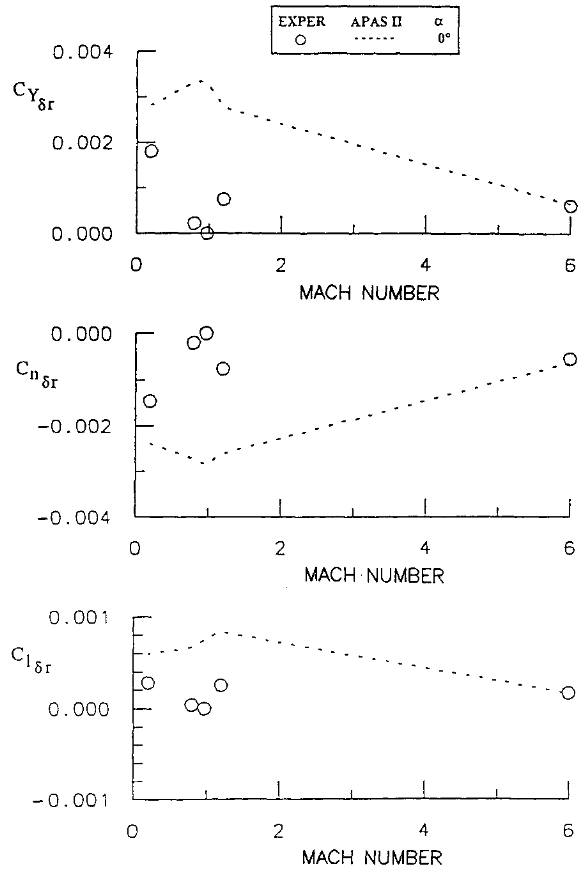

Fig. 10 Comparison of experimental and theoretical rudder effectiveness as a function of Mach number for the HRA.

dicted using UDP are in agreement with wind-tunnel and flight-test data.

Using similar results for all of the vehicles and flight conditions given in Table 2, fully detailed and discussed in Refs. 10 and 11, the suitability of the methods discussed for predicting the lateral/directional aerodynamics of interest for flight controls applications are summarized in Table 4. It is found that the lateral/directional derivatives are found to be better when shielding is not included in the calculations. In addition, at subsonic speeds, lateral control results are generally found to be better when the leading-edge suction force is included and the side-edge suction force is not.

The limitations of the theory, in particular the fact that separation effects are not taken into account, cause greater difficulties for the lateral/directional derivatives than in the case of the longitudinal derivatives. The theory is not able to predict aerodynamic behavior at extreme vehicle orientations, where portions of a surface or the entire surface can be blanketed in separated flow. This obviously leads to some nonlinearities in the control effectiveness not being taken into account and situations can be anticipated for which the prediction is not entirely satisfactory.

Summary of Predictions

Given that for conceptual design work the tradeoff between accuracy and speed of computation leans very heavily toward speed, all of the prediction methods contained in APAS are reasonable. It should be noted, however, that in the case of the subsonic and supersonic methods, a great deal of flexibility exists in balancing the tradeoff between accuracy and speed. The panel methods considered are basically as fast and robust as possible at the expense of accuracy. If more accuracy is desired, a number of improvements are possible between panel methods and a full-blown Navier-Stokes computation. For example, a more complete boundary-layer model could improve the drag predictions and, combined with empirical correlations, could greatly improve the derivatives strongly influenced by separation effects. If better accounting for the effects of compressibility is required, the flowfield could be modeled using the Euler equations rather than the linearized potential equation.

Whereas in the case of subsonic and supersonic Mach numbers there is a great deal of flexibility for achieving a desired level of accuracy by implementing a sufficiently rigorous theoretical model, this is not the case in the hypersonic flight regime. Essentially, there are no intermediate theoretical models between the simple flow inclination methods contained in HABP and full Euler or Navier-Stokes computation. Unfortunately at present, the time required for setting up computational grids, as well as execution requirements, are much too great for the full computational methods to be routinely used for conceptual design activities. Thus, methods such as those contained in HABP will likely remain the primary tools for preliminary flight control force and moment prediction for some time. For such work these methods can be expected to provide reasonable estimates provided they are applied to situations not dominated by strong viscous/inviscid interactions, real gas and/or rarefied gas effects, or flowfields containing extensive regions of separated flow.

Conclusions

This paper discussed the suitability of the methods contained in the Aerodynamic Preliminary Analysis System program for flight control force and moment predictions. In considering these results, it is concluded that, provided the results are interpreted carefully and major decisions are not based on predictions which are known to be suspect, all of the longitudinal results can be of some use in conceptual design studies. As expected, the most questionable calculations are those in which neglected separated flow can significantly influence the results. In the case of predicting lateral/directional control derivatives, some results are found to be unacceptable. Fortunately, however, the primary control derivatives $C_{l\delta_a}$ and $C_{n\delta_v}$ are found to provide reasonable results.

Acknowledgments

This research was supported by the Aircraft Guidance and Controls Branch, Guidance and Controls Division, NASA Langley Research Center under Grant NAG 1-849. The efforts and contributions of the technical monitors John D. Shaughnessy and David L. Raney are gratefully acknowledged.

References

[1]Bonner, E., Clever, W., and Dunn, K., "Aerodynamic Preliminary Analysis System II-Part I, Theory," NASA CR-165627, April 1981.

[2]Sova, G., and Divan, P., "Aerodynamic Preliminary Analysis System II-Part II, User's Manual," North American Aircraft Operations, Rockwell International, Los Angeles, CA, 1988.

[3]Woodward, F., "Analysis and Design of Wing-Body Combinations at Subsonic and Supersonic Speeds," *Journal of Aircraft*, Vol. 5, No. 6, 1968, pp. 528–534.

[4]Gentry, A. E., "Hypersonic Arbitrary-Body Aerodynamic Computer Program (Mark III Version). Vol. I—User's Manual," McDonnell Douglas Corp., Rept. DAC 61552, St. Louis, MO, April 1968.

[5]Middleton, W. D., Lundry, J. L., and Coleman, R. G., "A System for Aerodynamic Design and Analysis of Supersonic Aircraft, Part I–General Description and Development," NASA CR 3351, Dec. 1980.

[6]Fisher, C. M. E., "Experience Using the Mark IV Supersonic Hypersonic Arbitrary Body Program," *Aerodynamics of Hypersonic Lifting Vehicles*, AGARD CP-428, No. 31, April 1987.

[7]Covell, P. F., Wood, R. M., Bauer, S. X., and Malker, I. J., "Configuration Trade and Code Validation Study on a Conical Hypersonic Vehicle," AIAA Paper 88-4505, Sept. 1988.

[8]Moore, M. E., and Williams, J. E., "Aerodynamic Prediction Rationale for Analyses of Hypersonic Configurations," AIAA Paper 89-0525, Jan. 1989.

[9]Cruz, C. I., and Wilhite, A. W., "Prediction of High-Space Speed Aerodynamic Characteristics Using the Aerodynamic Preliminary Analysis System (APAS)," AIAA Paper 89-2173, Aug. 1989.

[10]Ozoroski, L. P., "Evaluation of Methods for Predicting the Forces and Moments Generated by Control Surface Deflections on Hypersonic Vehicles," M.S. Thesis, Dept. of Aerospace Engineering, Pennsylvania State University, University Park, PA, May 1990.

[11]Maughmer, M. D., Ozoroski, L. P., Straussfogel, D. M., and Shaughnessy, J. D., "Validation of Prediction Methods for Hypersonic Vehicle Control Effectors," NASP CR 1104, Jan. 1991.
[12]Anderson, J., *Hypersonic Flow and High Temperature Gas Dynamics*, McGraw-Hill, New York, 1989.
[13]Boisseau, P. C., "Investigation of the Low-Speed Stability and Control Characteristics of a 1–7 Scale Model of the North American X-15 Airplane," NACA RM L57D09, June 1957.
[14]McKinney, R. L., and Lancaster, J. A., "Investigation of the Aerodynamic Characteristics of a 0.02-Scale Model of the X-15 Airplane at Mach Numbers of 2.96, 3.96, and 4.65 at High Angles of Attack," NASM TM X-820, June 1963.
[15]Osbourne, R. S., "Aerodynamic Characteristics of a 0.0667-Scale Model of the N.A. X-15 Research Airplane at Transonic Speeds," NASA TM X-24, Sept. 1959.
[16]Penland, J. A., and Fetterman, D. E., Jr., "Static Longitudinal, Directional, and Lateral Stability and Control Data at a Mach Number of 6.83 of the Final Configuration of the X-15 Research Airplane," NASA TM X-236, April 1960.
[17]Yancey, R. B., Rediess, H. A., and Robinson, G. H., "Aerodynamic-Derivative Characteristics of the X-15 Research Airplane as Determined From Flight Tests for Mach Numbers from 0.6 to 3.4," NASA TN D-1060, Jan. 1962.
[18]Yancey, R. B., "Flight Measurements of Stability and Control Derivatives of the X-15 Research Airplane to a Mach Number of 6.02 and an Angle of Attack of 25 °," NASA TN D-2532, Nov. 1964.
[19]Penland, J. A., Dillon, J. L., and Pittman, J. L., "An Aerodynamic Analysis of Several Hypersonic Research Airplane Concepts from M=0.2 to 6.0," AIAA Paper 78-0150, Jan. 1978.
[20]Dillon, J. L., and Pittman, J. L., "Aerodynamic Characteristics at Mach Numbers from 0.33 to 1.20 of a Wing-Body Design Concept for a Hypersonic Research Airplane," NASA TP-1044, Dec. 1977.
[21]Dillon, J. L., and Creel, T. R., Jr., "Aerodynamic Characteristics at Mach Number 0.2 of a Wing-Body Concept for a Hypersonic Research Airplane," NASA TP-1189, June 1978.
[22]Dillon, J. L., and Pittman, J. L., "Aerodynamic Characteristics at Mach 6 of a Wing-Body Concept for a Hypersonic Research Airplane," NASA TP-1249, Aug. 1978.
[23]"Aerodynamic Design Data Book, Vol. I, Orbiter Vehicle STS-1," edited by W. R. Russel, Space Div., Rockwell International, SD72-SH-0060, Downey, CA, 1980.
[24]Maughmer, M., Ozoroski, L., Straussfogel, D., and Long, L.,"Validation of Engineering Methods for Predicting Hypersonic Vehicle Controls Forces and Moments," *Proceedings of the AIAA Atmospheric Flight Mechanics Conference* (New Orleans), AIAA, Washington DC, 1991, pp. 1–16 (AIAA Paper 91-2845).